Atomic Resolution X-ray Standing Wave Microstructural Characterization of NLO-Active Self-Assembled Chromophoric Superlattices

Wenbin Lin,[†] Tien-Lin Lee,[‡] Paul F. Lyman,[‡] Jaejin Lee,[§] Michael J. Bedzyk,*[,‡,⊥] and Tobin J. Marks*[,†,∥]

Contribution from the Department of Chemistry, Department of Materials Science, Department of Physics and Astronomy, and Materials Research Center, Northwestern University, Evanston, Illinois 60208-3113, and Materials Science Division, Argonne National Laboratory, Argonne, Illinois 60439

Received July 5, 1996[⊗]

Abstract: This contribution reports the first X-ray standing wave structural characterization of self-assembled NLO-active chromophoric multilayers (SAMs). These siloxane-based self-assembled stilbazolium multilayers are intrinsically acentric and exhibit very large second-order nonlinear optical responses. The locations of bromide ions within the SAMs were precisely determined using X-ray standing waves generated by total external reflection from mirror surfaces as well as by Bragg diffraction from layered synthetic microstructures. The large coherent fraction (i.e., small Gaussian distribution width) of the Br^- ions provides direct evidence for the high structural regularity of these self-assembled multilayers along the surface normal direction. These results are supported by atomic force microscopic (AFM) and X-ray photoelectron spectroscopic (XPS) studies which probe the structural regularity and chemical composition of SAMs, respectively. The *anion* surface coverage has also been measured in this study ($2.5(5) \times 10^{14}$ Br^-/cm^2) and is in excellent agreement with the *cation* surface coverage measured by second harmonic generation ($2(1) \times 10^{14}$ molecules/cm^2). These results clearly demonstrate the utility of X-ray standing wave analyses as a quantitative microstructural probe for self-assembled mono- and multilayers, especially for SAMs with incommensurate structures.

Introduction

Self-assembled monolayers and multilayers (SAMs) have attracted much attention in recent years, not only because of fundamental scientific interest but also because of potential technologies perceived for these artificially-structured thin-film materials.[1] Among the numerous adsorbate/substrate systems, thiols and sulfides on gold,[1,2] trichloro- and trialkoxysilanes on silicon oxide,[1,3] and alkylphosphonates on metal phosphonates[1,4] have been most extensively investigated. While a large body of spectroscopic and structural data are now available for the former system,[1,2] relatively little precise microstructural information has been obtained on the latter two systems due to their inherently incommensurate nature. In fact, low-angle X-ray reflectivity and atomic force microscopy (AFM) have so far been the only two quantitative metrical probes available for self-assembled films composed of trichloro- and trialkoxysilanes on silicon oxide and alkylphosphonates on metal phosphonates.[5,6] On the other hand, the X-ray standing wave (XSW) technique has recently proven to be a powerful structural probe for adsorbed surface layers by virtue of the ability to define features above a surface.[7] For example, long-period XSWs generated by total external reflection (TER) from X-ray mirror surfaces and by Bragg diffraction from layered synthetic microstructures (LSM) have been used to determine the positions of heavy atoms in Langmuir-Blodgett (LB) films as well as in chemisorbed overlayers at electrochemical interfaces.[8] The present contribution reports the first application of the long-period X-ray standing wave (XSW) technique to self-assembled mono- and multilayers, which probes the structural regularity of these SAMs along the surface normal direction.

We have recently developed a self-assembly approach to constructing intrinsically acentric, structurally regular chromophoric superlattices which exhibit very large second-order nonlinear optical (NLO) responses.[5d,9] The assembly of these superlattices involves sequential deposition of a silane coupling layer, a stilbazolium chromophore layer, and an octachloro-

[†] Department of Chemistry, Northwestern University.
[‡] Department of Materials Science, Northwestern Univrsity.
[§] Department of Physics and Astronomy, Northwestern University.
[⊥] Materials Science Division, Argonne National Laboratory.
[∥] Materials Research Center, Northwestern University.
[⊗] Abstract published in *Advance ACS Abstracts,* January 15, 1997.

(1) (a) Ulman, A. *An Introduction to Ultrathin Organic Films*; Academic Press: New York, 1991; Part 3. (b) Swalen, J. D.; Allara, D. L.; Andrade, J. D.; Chandross, E. A.; Caroff, S.; Israelachvili, J.; McCarthy, T. J.; Murray, R.; Pease, R. F.; Rabolt, J. F.; Wynne, K. J.; Yu, H. *Langmuir* **1987**, *3*, 932−950. (c) Dubois, L. H.; Nuzzo, R. G. *Annu. Rev. Phys. Chem.* **1992**, *43*, 437−463. (d) Bell, C. M.; Yang, H. C.; Mallouk, T. E. In *Materials Chemistry: An Emerging Discipline*; Interrante, L. V., Casper, L. A., Ellis, A. B., Eds.; Adv. Chem. Ser. 245, American Chemical Society: Washington, D.C., 1995; pp 212−230. (e) Ulman, A. *Chem. Rev.* **1996**, *96*, 1533−1554.

(2) (a) Nuzzo, R. G.; Allara, D. L. *J. Am. Chem. Soc.* **1983**, *105*, 4481−4483. (b) Nuzzo, R. G.; Fusco, F. A.; Allara, D. L. *J. Am. Chem. Soc.* **1987**, *109*, 2358−2368. (c) Bain, C. D.; Whitesides, G. M. *Angew. Chem., Int. Ed. Engl.* **1989**, *28*, 506−512. (d) Bain, C. D.; Troughton, E. B.; Tao, Y.-T.; Evall, J.; Whitesides, G. M.; Nuzzo, R. G. *J. Am. Chem. Soc.* **1989**, *111*, 321−335. (e) Gerdy, J. J.; Goodard, III, W. A. *J. Am. Chem. Soc.* **1996**, *118*, 3233−3236. (f) Chailapakul, O.; Sun, L.; Xu, C.; Crooks, R. M. *J. Am. Chem. Soc.* **1993**, *115*, 12459−12467.

(3) (a) Wasserman, S. R.; Tao, Y.-T.; Whitesides, G. M. *Langmuir* **1989**, *5*, 1074−1087. (b) Maoz, R.; Sagiv, J. *Langmuir* **1987**, *3*, 1034−1044. (c) Pomerantz, M.; Segmuller, A.; Netzer, L.; Sagiv, J. *Thin Solid Films* **1985**, *132*, 153−162. (d) Stenger, D. A.; Georger, J. H.; Dilcey, C. S.; Hickman, J. J.; Rudolph, A. S.; Nielsen, T. B.; McCort, S. M.; Calvert, J. M. *J. Am. Chem. Soc.* **1992**, *114*, 8435−8442.

(4) (a) Katz, H. E.; Scheller, G.; Putvinscki, T. M.; Schilling, M. L.; Wilson, W. L.; Chidsey, C. E. D. *Science* **1991**, *254*, 1485−1487. (b) Katz, H. E.; Wilson, W. L.; Scheller, G. *J. Am. Chem. Soc.* **1994**, *116*, 6636−6640. (c) Zeppenfeld, A. C.; Fiddler, S. L.; Ham, W. K.; Klopfenstein, B. J.; Page, C. J. *J. Am. Chem. Soc.* **1994**, *116*, 9158−9165. (d) Cao, G.; Hong, H.-G.; Mallouk, T. E. *Acc. Chem. Res.*, **1992**, *25*, 420−425. (e) Thompson, M. E. *Chem. Mater.* **1994**, *6*, 1168−1175.

S0002-7863(96)02293-7 CCC: $14.00

Scheme 1. Siloxane-Based Self-Assembly Approach to the Construction of Intrinsically Acentric, Highly Regular Stilbazolium Superlattices

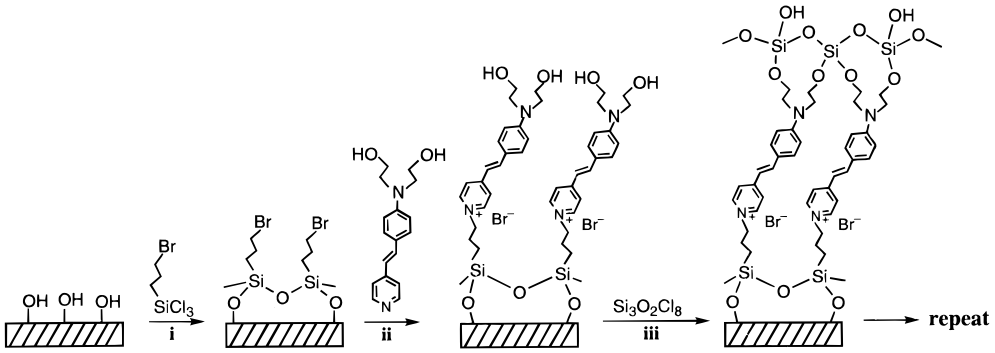

trisiloxane capping layer (Scheme 1). This approach allows the incorporation of varying chromophore modules as well as accommodation of different counteranions as a result of the salt-like structure of these assemblies. Heavy halide atoms such as bromine and iodine provide excellent X-ray fluorescence probes with which the microstructural characterization of these self-assembled multilayers becomes possible using X-ray standing waves; the XSW technique is capable of locating heavy atoms with atomic resolution along the surface normal direction of the substrate.[7,8] More importantly, recent experimental and theoretical results indicate that the NLO responses of self-assembled stilbazolium structures are strongly dependent on the nature and location of these counteranions. For example, exchange of chloride with iodide within these monolayers leads to significant increases in the response, presumably because the incoming iodide ions occupy spatially different positions with respect to the stilbazolium cation than those of the displaced chloride anions.[10] In this regard, the ability to accurately determine the spatial distribution of these halide counterions is crucial to delineating structure/property/NLO response relationships in self-assembled mono- and multilayers. To this end, we have undertaken the first XSW study on self-assembled stilbazolium mono- and multilayers constructed from trichlorosilanes on silicon oxide, which pinpoints the locations of halide anions within the SAMs with atomic resolution. These results are supported by atomic force microscopic (AFM) and X-ray photoelectron spectroscopic (XPS) studies which probe the in-plane structural regularity and the chemical composition of the SAMs, respectively.

Experimental Section

Synthesis. The synthesis of the coupling agent 3-iodopropyltrichlorosilane (3-$IC_3H_6SiCl_3$) and the deposition of self-assembled coupling and capping layers were carried out under rigorously anhydrous/anaerobic conditions. Pentane (Fisher Scientific) and heptane (Fisher Scientific) were distilled from Na/K alloy before use. The reagent 3-bromopropyltrichlorosilane (United Chemical Technologies) was purified by vacuum distillation. The coupling agent 3-$IC_3H_6SiCl_3$ was prepared by stirring excess dry NaI (200 mmol) and 1.4 mL 3-bromopropyltrichlorosilane (8.8 mmol) in anhydrous (distilled from CaH_2 under N_2) acetonitrile (30 mL) for 8 h. The resulting 3-$IC_3H_6SiCl_3$ was extracted into dry heptane and used *in situ* for coupling agent deposition. This type of halogen metathesis reaction has previously been used to prepare benzylic iodide compounds.[9a,11] The completion of this metathesis reaction was also verified by X-ray photoelectron spectroscopy; the spectrum of the coupling layer prepared with 3-$IC_3H_6SiCl_3$ shows no detectable Br 3d signal (normally at ~70 eV for a bromoalkane functionality).[12]

Self-assembled samples for X-ray photoelectron spectroscopic (XPS) and atomic force microscopic (AFM) measurements were deposited on N-doped silicon (001) wafers (Semiconductor Processing Company), while the SAMs for XSW measurements were adsorbed on the surface of a periodic Si/Mo layered-synthetic microstructure (LSM) (Ovonyx). The layered synthetic microstructures (LSMs) used in this study consisted of 60 layer pairs of molybdenum and silicon grown on a silicon wafer, with Si as the top layer. The layer pairs have a molybdenum layer thickness of 15.9 Å and a silicon layer thickness of 20.6 Å, corresponding to a total periodicity of $d = 36.5$ Å. Due to the growth of native silicon oxide, the thickness of the top Si layer is increased to 28 Å as determined by combining our TER (total external reflection)-XSW and Bragg-XSW results.

Silicon wafer substrates were cleaned by immersion in "piranha" solution (c H_2SO_4:30% H_2O_2 70:30 v/v) at 80 °C for 1 h and sonication in an RCA-type cleaning solution (H_2O:30% H_2O_2:NH_3 5:1:1 v/v/v) at room temperature for 40 min. The substrates were then washed with copious amounts of deionized water and dried under vacuum immediately before coupling agent deposition. The Si/Mo LSM substrates were cleaned by repeated sonication in 1,1,1-trichloroethane and acetone.

(5) (a) Wasserman, S. R.; Whitesides, G. M.; Tidswell, I. M.; Ocko, B. M.; Pershan, P. S.; Axe, J. D. *J. Am. Chem. Soc.* **1989**, *111*, 5852−5861. (b) Maoz, R.; Sagiv, J.; Degenhardt, D.; Mohwald, H.; Quint, P. *Supramolecular Science* **1995**, *1*, 9−24. (c) Roscoe, S. B.; Kakkar, A. K.; Marks, T. J.; Malik, A.; Durbin, M. K.; Lin, W.; Wong, G. K.; Dutta, P. *Langmuir* **1996**, *12*, 4218−4223. (d) Lin, W.; Lin, W.; Wong, G. K.; Marks, T. J. *J. Am. Chem. Soc.* **1996**, *118*, 8034−8042.

(6) (a) Bierbaum, K.; Grunze, M.; Baski, A. A.; Chi, L. F.; Schrepp, W.; Fuchs, H. *Langmuir* **1995**, *11*, 2143−2150. (b) Caldwell, W. B.; Campbell, D. J.; Chen, K.; Herr, B. R.; Mirkin, C. A.; Malik, A.; Durbin, M. K.; Dutta, P.; Huang, K. G. *J. Am. Chem. Soc.* **1995**, *117*, 6071−6081. (c) Fujii, M.; Sugisawa, S.; Fukada, K.; Kato, T.; Shirakawa, T.; Seimiya, T. *Langmuir* **1994**, *10*, 984−987. (d) Alves, C. A.; Smith, E. L.; Porter, M. D. *J. Am. Chem. Soc.* **1992**, *114*, 1222−1227. (e) Yang, H. C.; Aoki, K.; Hong, H.-G.; Sackett, D. D.; Arendt, M. F.; Yau, S.-L.; Bell, C. M.; Mallouk, T. E. *J. Am. Chem. Soc.* **1993**, *115*, 11855−11862. (f) Byrd, H.; Snover, I. L.; Thompson, M. E. *Langmuir* **1995**, *11*, 4449−4453.

(7) (a) Cowan, P. L.; Golovchenko, J. A.; Robbins, M. F. *Phys. Rev. Lett.* **1980**, *44*, 1680−1683. (b) Golovchenko, J. A.; Patel, J. R.; Kaplan, D. R.; Cowan, P. L.; Bedzyk, M. J. *Phys. Rev. Lett.* **1982**, *49*, 560−563. (c) Bedzyk, M. J.; Materlik, G. *Phys. Rev.* **1985**, *B31*, 4110−4112.

(8) (a) Bedzyk, M. J.; Bilderback, D. H.; Bommarito, G. M.; Caffrey, M.; Schildkraut, J. S. *Science* **1988**, *241*, 1788−1791. (b) Bedzyk, M. J.; Bommarito, G. M.; Schildkraut, J. S. *Phys. Rev. Lett.* **1989**, *62*, 1376−1379. (c) Wang, J.; Bedzyk, M. J.; Penner, T.; Caffrey, M. *Nature* **1991**, *254*, 377−380. (d) Abruna, H. D.; Bommarito, G. M.; Acevedo, D. *Science* **1990**, *250*, 69−74. (e) Abruna, H. D.; Bommarito, G. M.; Yee, H. S. *Acc. Chem. Res.* **1995**, *28*, 273−279.

(9) (a) Li, D.; Ratner, M. A.; Marks, T. J.; Zhang, C.; Yang, J.; Wong, G. K. *J. Am. Chem. Soc.* **1990**, *112*, 7389−7390. (b) Kakkar, A. K.; Yitzchaik, S.; Roscoe, S. B.; Kubota, F.; Allan, D. S.; Marks, T. J.; Lin, W.; Wong, G. K. *Langmuir* **1993**, *9*, 388−390. (c) Lin, W.; Yitzchaik, S.; Lin, W.; Malik, A.; Durbin, M. K.; Richter, A. G.; Wong, G. K.; Dutta, P.; Marks, T. J. *Angew. Chem., Int. Ed. Engl.* **1995**, *34*, 1497−1499. (d) Yitzchaik, S.; Marks, T. J. *Acc. Chem. Res.* **1996**, *29*, 197−202.

(10) (a) Roscoe, S. B.; Yitzchaik, S.; Kakkar, A. K.; Marks, T. J.; Lin, W.; Wong, G.K. *Langmuir* **1994**, *10*, 1337−1339. (b) Roscoe, S. B.; Yitzchaik, S.; Kakkar, A. K.; Marks, T. J.; Xu, Z.; Zhang, T.; Lin, W.; Wong, G. K. *Langmuir* **1996**, *12*, 5338−5349. (c) Di Bella, S.; Fragala, I.; Ratner, M. A.; Marks, T. J. *Chem. Mater.* **1995**, *7*, 400−404.

(11) Koloski, T. S.; Dulcey, C. S.; Haralson, Q. J.; Calvert, J. M. *Langmuir* **1994**, *10*, 3122−3133.

(12) Moulder, J. F.; Stickle, W. F.; Sobol, P. E.; Bomben, K. D. *Handbook of X-ray Photoelectron Spectroscopy*; Perkin Elmer: Eden Praire, MN, 1992.

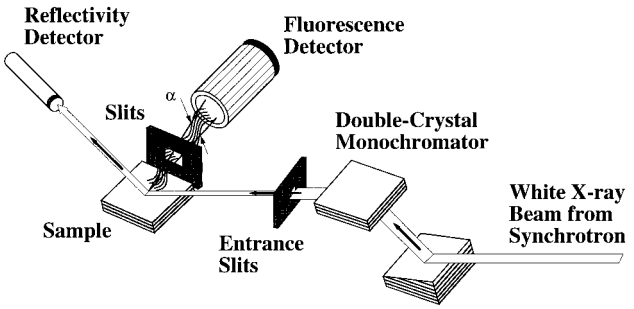

Figure 1. Schematic of the experimental setup for X-ray standing wave measurements.

(i) Self-Assembly of 3-Bromopropyltrichlorosilane. Under inert atmosphere, the freshly cleaned substrates were immersed in a 1:100 (v/v) solution of 3-$BrC_3H_6SiCl_3$ in heptane for 20 min, washed with copious amounts of pentane, and sonicated in acetone for 1 min. The 3-$IC_3H_6SiCl_3$ coupling layers were similarly chemisorbed.

(ii) Self-Assembly of the [4-*N*,*N*-Bis(hydroxylethyl)amino]stilbazolium Chromophore. The silylated substrates (after step (i) treatment) were spin-coated at 4000 rpm with a 5 mM solution of [4-*N*,*N*-bis-(hydroxylethyl)amino]stilbazole in methanol inside a class 100 clean hood (Envirco) and then heated at 130 °C in a vacuum oven (0.4 Torr) for 25 min. The samples were cooled to room temperature and then washed with copious amounts of methanol and acetone to remove any residual stilbazole.

(iii) Self-Assembly of Octachlorotrisiloxane. The substrates after steps i and ii treatment were immersed in a 1:150 (v/v) solution of octachlorotrisiloxane in heptane for 30 min, washed with copious amounts of pentane, and sonicated in acetone for 1 min.

Physical Measurements. (i) X-ray standing wave. The XSW experiments were carried out at beamline X15A of the National Synchrotron Light Source (NSLS) at Brookhaven National Laboratory (Figure 1). The white synchrotron radiation was monochromated with a pair of Ge(111) crystals to an X-ray energy of 13.6 keV for exciting Br K fluorescence. The SAM/LSM samples were aligned on a two-circle diffractometer to reflect in the vertical plane, and throughout the X-ray experiments, the samples were contained within a helium-filled cell having polypropylene windows. A solid state Si (Li) detector was located perpendicular to the vertical scattering plane to collect the Br fluorescence emission at a glancing angle with respect to the sample surface (Figure 1). A Si photodiode detector was located in the 2θ scattering direction for measuring the reflectivity. The fluorescence yield from the Br atoms within the SAMs was monitored while scanning the incident angle θ through both the TER and first-order Bragg reflection.

(ii) XPS and AFM. X-ray photoelectron spectra were recorded on a VG Scientific Ltd., Escalab MK II instrument with a monochromatic Al source at 1486.6 eV. The details of the spectral acquisition and data analysis techniques were reported previously.[10a] Atomic force microscopic images were recorded using a Nanoscope II microscope with A and D scanners (Digital Instruments, Inc.). All samples were prepared on Si(001) single crystal substrates having an RMS roughness of 2.0 Å. All the images were obtained in air with Si_3N_4 cantilevers having pyramidal tips with 70° cone angles and 20−50 nm radii of curvature. The cantilevers had force constants of 0.58 N/m. The images were acquired in the height mode with a total force of 20−60 nN and a scan rate of ~10 Hz. The authenticity of the images was verified by scanning the same area several times to ensure reproducibility as well as by scanning different area sizes (i.e., at different magnifications) to examine image consistency. All the RMS roughness values are reported in an area of 1 μm^2.

Results and Discussion

The self-assembled stilbazolium films were grown on native silicon oxide via the iterative deposition of three layer-building steps (Scheme 1): step (i) introduces an alkyl halide functionality onto the surface through spontaneous chemisorption of coupling agents such as 3-$BrCH_2CH_2CH_2SiCl_3$ (coupling layer);

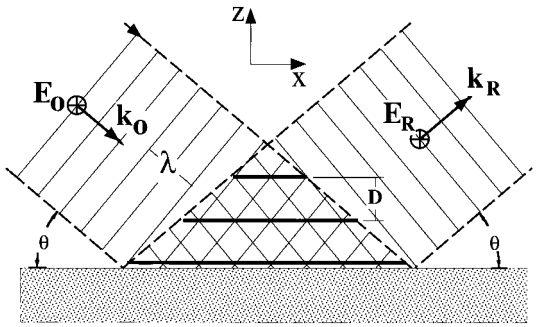

Figure 2. Illustration of the X-ray standing wave field generated by the interference of an incident and reflected plane wave.

step (ii) self-assembles a monolayer of high-hyperpolarizability stilbazolium chromophore molecules via a quaternization reaction (chromophore layer); and finally, step (iii) cross-links the stilbazolium molecules with octachlorotrisiloxane (capping layer), which not only stabilizes the polar order but also provides active sites for subsequent layer deposition.[5d,9c] In this section, the X-ray standing wave (XSW) studies of these self-assembled samples will be first reported, followed by the results of atomic force microscopic (AFM) and X-ray photoelectron spectroscopic studies.

X-ray Standing Wave Studies. To investigate the microstructures of these self-assembled films, XSW measurements were performed on three sets of samples: sample **1** having a self-assembled (3-bromopropyl)trichlorosilane monolayer, sample **2** having a complete (3-bromopropyl)trichlorosilane, 4-*N*,*N*-bis-(hydroxyethylamino)stilbazolium chromophore, and octachlorotrisiloxane trilayer, and sample **3** having two complete trilayers with (3-iodopropyl)trichlorosilane as the coupling layer in the bottom trilayer and (3-bromopropyl)trichlorosilane in the top trilayer.

As depicted in Figure 2, the XSW is produced in a reflection geometry by the interference between the incident and specularly reflected X-ray plane waves. In the present case, a sufficiently intense reflected beam is generated by (1) Bragg diffraction from the layered synthetic microstructures (LSM)[8a] and (2) total external reflection (TER) from the X-ray mirror surface[8b] of the LSM. In either case, the antinodal planes of the XSW are parallel to the surface-interface and have a period of $D = \lambda/(2\sin\theta)$. The E-field intensity above the reflecting surface can be described as

$$I(\theta,z) = |E_o|^2[1 + R(\theta) + 2\sqrt{R(\theta)}\cos(\upsilon(\theta) - 2\pi Qz)] \quad (1)$$

where $Q = 2\sin\theta/\lambda = 1/D$ is the magnitude of the wave-vector transfer $\mathbf{Q} = \mathbf{k_R} - \mathbf{k_0}$. The modulation of the E-field intensity in the XSW (eq 1) is sufficiently strong for probing atomic positions via fluorescence when the reflectivity (R) approaches unity. This occurs at small incident angles ($0 < \theta < \theta_c$) due to total external reflection (TER) as well as in a narrow angular region surrounding the first-order Bragg diffraction peak. While the TER-XSW period varies inversely with angle θ and reduces to about 100 Å at the critical angle (θ_c), the Bragg-XSW period is essentially fixed to the LSM period (d) which is much closer to the nanometer length-scale of the SAMs. In addition to the amplitude and period, one also needs to describe the XSW phase (υ), which diminishes by π radians as θ is scanned through each of the strong reflections. For the TER-XSW case, this causes the E-field intensity at the mirror surface $I(\theta,0)$ to change from nodal to antinodal as θ is scanned from 0 to θ_c. For the Bragg-XSW case, scanning through the strong Bragg diffraction condition causes the antinodal planes of the XSW to move inward by one-half of a period (d-spacing) with the antinodes

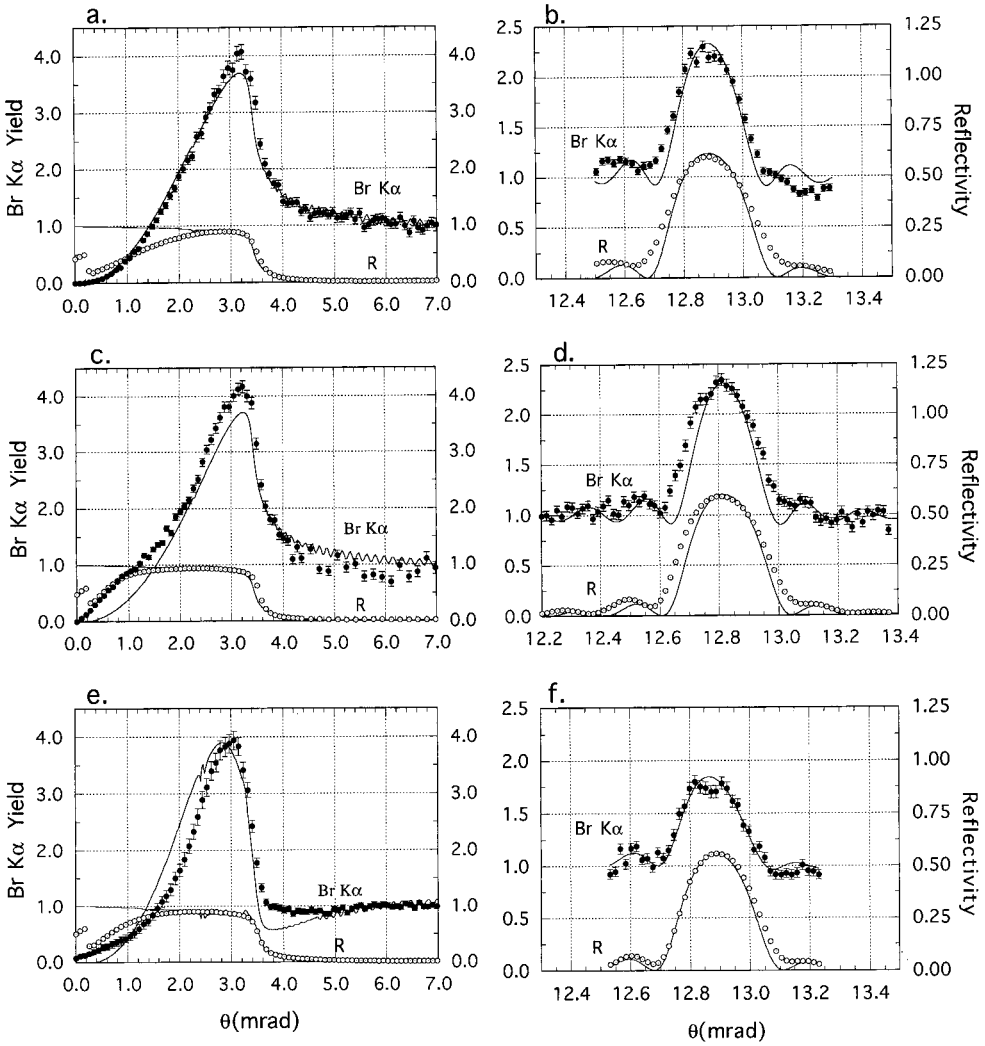

Figure 3. Experimental data and theoretical curves for Br K_α fluorescence yield and reflectivity versus incident angle θ. The solid circles and open circles represent experimental Br K_α fluorescence yield and reflectivity, respectively, and the solid curves are the theoretical fits to the experimental data. From the fit of eq 3 to the Bragg-XSW experimental data, the coherent position (P) and coherent fraction (f_c) can be obtained (see Table 1). The monochromatic X-ray beam has an energy of 13.6 keV. Parts a, c, and e are the results from TER-XSW measurements on samples **1**, **2**, and **3**, respectively. Parts b, d, and f are the results from Bragg-XSW measurements on samples **1**, **2**, and **3**, respectively. The idealized structures for samples **1**−**3** are shown in Charts 1 and 2.

ending up in-phase with the centers of the higher density (Mo) layers on the high angle side. In the present XSW measurements, the fluorescence yield from the halide atoms within the SAMs was monitored while scanning θ through both the TER and first-order Bragg reflection. Analysis of the modulation curves affords a Fourier transform of the halide normalized distribution profile ($\rho(z)$) as projected along the surface normal direction (z). The dependence of the fluorescence yield on angle θ can be expressed as

$$Y(\theta) = \int_0^\infty \rho(z)\, I(\theta,z)\, dz \qquad (2)$$

For the Bragg reflection case, where the XSW period is essentially constant at $D = d$ (the diffraction plane spacing), the yield can be parameterized as

$$Y(\theta) = Y_{OB}[1 + R(\theta) + 2\sqrt{R(\theta)} f_c \cos(\nu(\theta) - 2\pi P)] \qquad (3)$$

where Y_{OB} is the off-Bragg fluorescence yield. The coherent fraction (f_c) and coherent position (P) represent the normalized amplitude and phase of the Fourier component of the spatial distribution of the fluorescent atom, respectively.[13] For simplicity, we model the distribution profiles ($\rho(z)$) for the halide atoms as Gaussians. In this case, the Bragg-XSW coherent position (P) is the Modulo-1 $\Delta d/d$ fractional d-spacing mean-position of the halide layer with respect to the diffraction planes. From our earlier definition of the phase of the XSW, the diffraction planes are defined by the centers of the high density layers in the diffracting multilayer. The Bragg-XSW coherent fraction can be interpreted in terms of the width (σ) of a Gaussian profile as

$$f_c = \exp(-2\pi^2\sigma^2 d^{-2}) \qquad (4)$$

The mean position and width are determined from the Bragg-XSW measurement with a typical resolution of $d/100$ which is 0.4 Å for the present LSM multilayer.

Based on eqs 1 and 2, it can be shown that the TER-XSW yield measures the Fourier transform of $\rho(z)$ over a continuous range in Q from 0 to $1/D_c$, where $D_c = \lambda/(2\theta_c)$, is the period at the critical angle[8b] (D_c = 130 Å for our LSM). This can lead directly to a determination of $\rho(z)$ at a 2 Å level of resolution.

Measured X-ray reflectivity (open circles) and Br K_α fluorescence yield (solid circles) data for samples **1**−**3** are shown in Figure 3. The solid curves are the best fits of eqs 2 and 3 to the experimental yield data using a Gaussian distribution model.

Chart 1

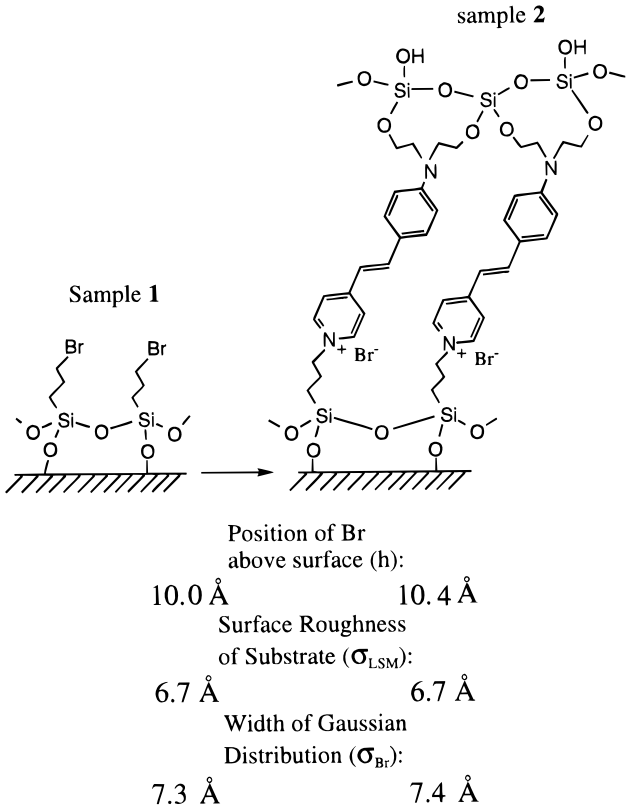

The theoretical reflectivity[13] are fitted to the reflectivity data in Figure 3 which is in turn parameterized by the electron density profile of the SAM/LSM to determine the values of the surface and interface roughness. For samples **1** and **2**, both TER-XSW and Bragg-XSW results can be reasonably fit to theoretical models (see Table 1 for detailed parameters). The Bragg-XSW fits reveal that the coherent position (P) and coherent fraction (f_c) for sample **1** are 0.25 and 0.45, respectively, translating into a mean height above the silicon oxide surface of 10.0 Å and a Gaussian distribution width of 7.3 Å (from eq 4) for the Br atoms in sample **1**. The calculated Br mean position above the surface is in excellent agreement with the thickness (∼10 Å) of the monolayers on silicon determined by X-ray reflectivity.[9c,14] Given that the LSMs have a surface roughness of ∼6 Å, the Gaussian distribution width of 7.3 Å indicates that the Br atoms within the monolayers are quite well-ordered along the z-direction, i.e., occur at a nearly uniform adsorption height. Interestingly, as the (3-bromopropyl)trichlorosilane monolayers undergo subsequent quaternization with 4-*N*,*N*-bis(hydroxyethylamino)stilbazole and then capping with octachlorotrisiloxane (sample **2**), *the coherent position and coherent fraction of the Br atoms remain essentially unchanged* (see Table 1). This result strongly argues that the present self-assembly approach is capable of producing highly regular superlattice structures.

TER- and Bragg- XSW measurements were also carried out on multilayer samples having *two trilayers* (sample **3**). In order to overcome the interference of Br fluorescence from two different trilayers, (3-iodopropyl)trichlorosilane was used as the coupling agent for the bottom trilayer and Br K_α fluorescence was monitored from the top trilayer which contained the (3-bromopropyl)trichlorosilane coupling layer. From the best fits of TER- and Bragg-XSW data to eqs 3 and 4 (Figure 3e and 3f), the Br mean position and Gaussian width were determined to be 48.4 Å and 10.4 Å, respectively. In a separate experiment, X-ray reflectivity was used to determine the trilayer thickness to be 34 ± 1 Å for the stilbazolium multilayer with (3-iodopropyl)trichlorosilane as the coupling agent.[14] According to the reflectivity results, the Br mean position in sample **3** would then be expected to be 44 ± 1 Å above the surface. The small discrepancy (∼4 Å) between the two experiments may be an artifact of the octachlorotrisiloxane layer deposition. We have noticed that the capping layer thickness is slightly sensitive to reagent history: octachlorotrisiloxane solutions tend to give slightly thicker films after multiple uses, presumably due to slight differences in extent of hydrolysis.[15] Additionally, the Br Gaussian distribution width in sample **3** is determined to be 10.4 Å, which is somewhat larger than those of samples **1** and **2**. This erosion of order is also likely a result of the aforementioned capping layer deposition artifact.[15] Interestingly, however, the capping layer is essential for maintaining the structural stability as well as acentricity of the stilbazolium multilayers.[5d,9c,15] In a previous study, we attempted to prepare chromophoric superlattices of the present type without the siloxane capping step (step (iii)).[15] Although optical spectroscopy and X-ray reflectivity measurements suggest the build-up of a structurally regular superlattice, the increase of the measured SHG intensity with the number of layers is not quadratic. When the number of layers exceeds three, the SHG intensity begins to decline. This result indicates that in the absence of the lateral stabilization imparted by step (iii), randomization of chromophore alignment, perhaps induced by chromophore dipole−dipole repulsions, destroys the microstructural acentricity. It

Chart 2

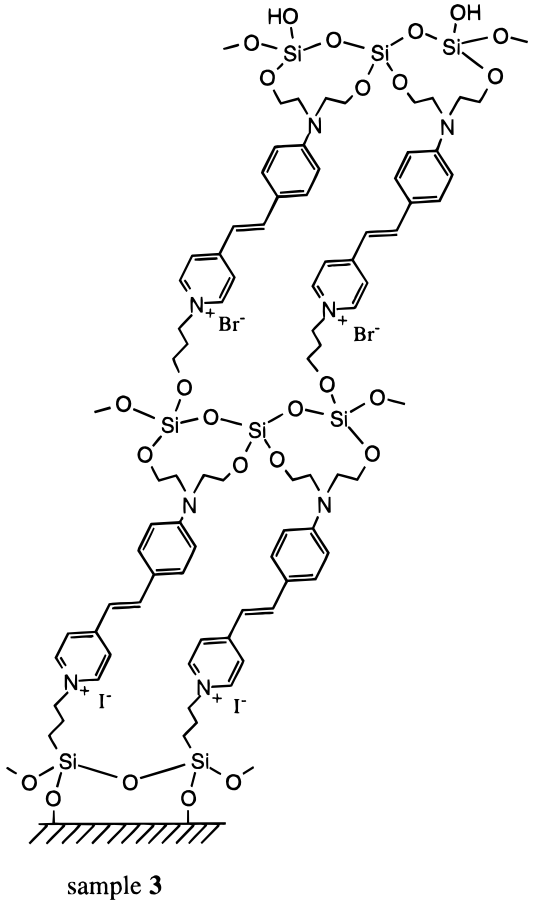

(13) Parratt, L. G. *Phys. Rev.* **1954**, *95*, 359−369.
(14) Malik, A; Lin, W.; Durbin, M. K.; Marks, T. J.; Dutta, P. *J. Chem. Phys.* In press.
(15) Lin, W.; Marks, T. J.; Yitzchaik, S.; Lin, W.; Wong, G. K. *Mat. Res. Soc. Sympos. Proc.* **1995**, *392*, 95−101.

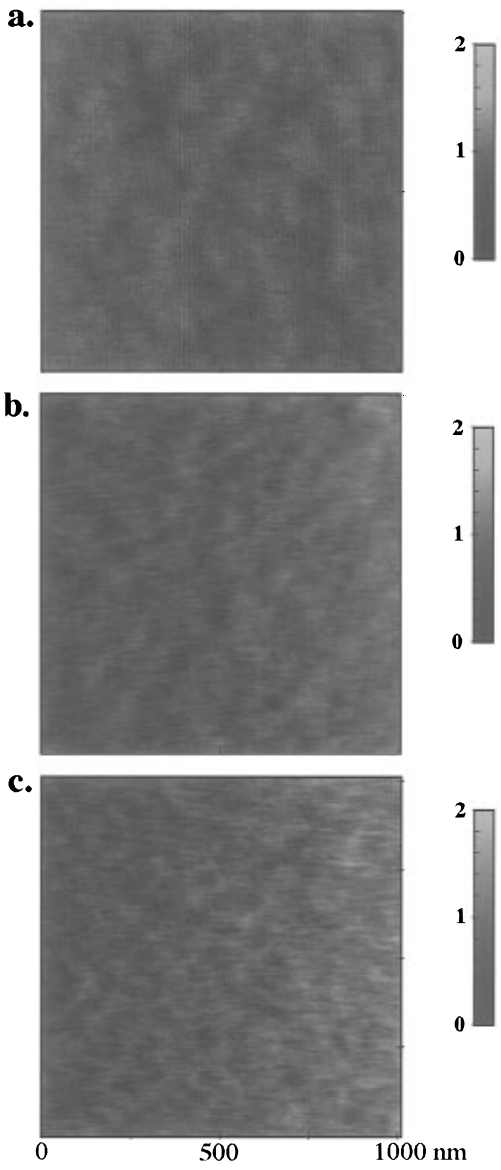

Figure 4. AFM images at 1 × 1 μm^2 scan area of self-assembled samples. (a) A self-assembled monolayer composed of 3-$BrC_3H_6SiCl_3$ coupling agent. Surface RMS roughness = 3.5 Å. (b) A self-assembled bilayer composed of 3-$BrC_3H_6SiCl_3$ coupling agent and stilbazolium chromophore. Surface RMS roughness = 4.0 Å. (c) A self-assembled trilayer composed of 3-$BrC_3H_6SiCl_3$ coupling agent, stilbazolium chromophore, and octachlorotrisiloxane capping agent. Surface RMS roughness = 5.2 Å.

is also interesting to note that the chromophoric superlattices built without step (iii) have higher optical absorption per layer than those of Scheme 1. This is consistent with a larger portion of the stilbazolium chromophores lying parallel to the surface as a result of loss of microstructural acentricity without the siloxane capping step.

Atomic Force Microscopic (AFM) Studies. In order to understand the surface morphologies of these self-assembled multilayers, we have also carried out AFM studies on these samples. The samples for AFM studies were grown on silicon wafer substrates with an RMS surface roughness of 2 Å. AFM shows that sample **1** has an RMS surface roughness of 3.5 Å; the 1.5 Å increase in surface roughness after the growth of a monolayer of 3-bromopropyltrichlorosilane on the wafer is rather small compared to the 10 Å thickness of the monolayer (Figure 4a). Upon quaternization with 4-*N*,*N*-bis(hydroxyethylamino)-stilbazole, the RMS surface roughness increases slightly to 4

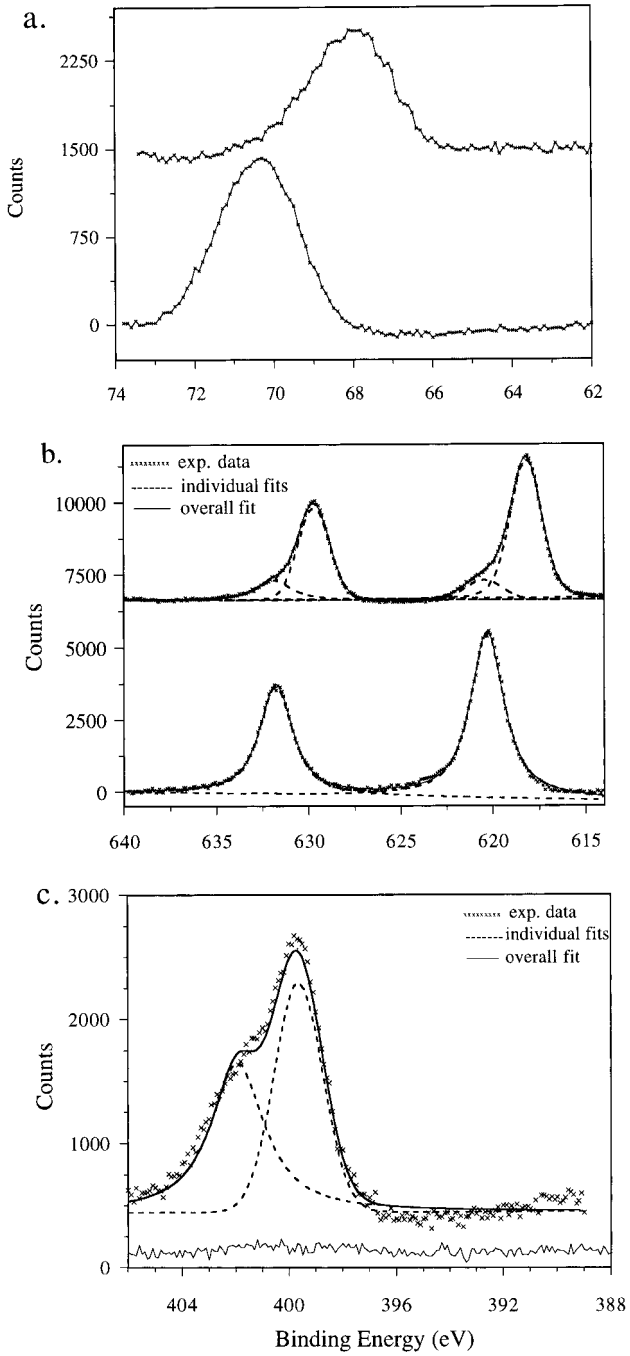

Figure 5. X-ray photoelectron spectra of self-assembled coupling and stilbazolium chromophore monolayers. (a) Br 3d XPS spectra of self-assembled monolayers with 3-$BrC_3H_6SiCl_3$ as the coupling agent. Bottom spectrum: after coupling agent deposition; top spectrum: after coupling agent and chromophore deposition. (b) I 3d XPS spectra of self-assembled monolayers with 3-$IC_3H_6SiCl_3$ as the coupling agent. Bottom spectrum: after coupling agent deposition; top spectrum: after coupling agent and chromophore deposition. (c) N 1s XPS spectra of a self-assembled stilbazolium monolayer. Bottom spectrum: after coupling agent deposition; top spectrum: after coupling agent and chromophore deposition.

Å for the bilayer structure consisting of (3-bromopropyl)-trichlorosilane coupling layer and 4-*N*,*N*-bis(hydroxyethylamino)stilbazolium chromophore layer (Figure 4b). After treatment with octachlorotrisiloxane, sample **2** exhibits a surface roughness of 5.2 Å (Figure 4c). The fact that all three of these samples show rather smooth morphologies further supports the high structural regularity of the superlattices produced by the present self-assembly approach.

Table 1. Metrical Parameters Obtained from Fitting the XSW Data Shown in Figure 3 to Eqs 2 and 3 with a Gaussian Model

sample	Bragg-XSW $(\Delta d/d)_{Br}$[a]	Bragg-XSW f_c[b]	Bragg-XSW h_{Br}[c] (Å)	Bragg-XSW σ_{Br}[d] (Å)	TER-XSW h_{Br}[c] (Å)	Θ_{Br}[e] (10^{14} Br/cm^2)
1	0.25	0.45	10.0	7.3	10	2.5 ± 0.5
2	0.26	0.45	10.4	7.4	10	
3	1.30	0.20	48.4	10.4	48	2.5 ± 0.5

[a] Coherent position. [b] Coherent fraction. [c] Mean Br position. [d] Width of Gaussian distribution. [e] Br coverage.

X-ray Photoelectron Spectroscopic (XPS) Studies. XPS provides additional information regarding the self-assembly chemistry. XPS spectra of sample **1** show a Br 3d signal at 70.5 eV, a binding energy consistent with an alkyl bromide moiety (Figure 5a).[12] Upon quaternization, the Br 3d binding energy shifts to 68.1 eV for the bilayer structure consisting of (3-bromopropyl)trichlorosilane coupling layer and 4-*N*,*N*-bis-(hydroxyethylamino)stilbazolium chromophore layer. This 2.4 eV shift to lower binding energy is consistent with the formation of Br^- anions.[12] As expected, the deposition of the octachlorotrisiloxane capping layer does not change the Br XPS binding energy, i.e., sample **2** exhibits a Br XPS spectrum identical to that of the above bilayer structure. Overlap of the Br $3d_{3/2}$ and Br $3d_{5/2}$ peaks complicates the deconvolution of the Br 3d signals and therefore precludes quantitative analysis of the extent of the quaternization process. This difficulty was overcome using $3\text{-}IC_3H_6SiCl_3$ as the coupling agent. Here, the I $3d_{5/2}$ and I $3d_{3/2}$ peaks are well separated by ~11.5 eV, and quantitative analysis of the $3d_{5/2}$ peaks becomes possible. While the monolayer sample with only the $3\text{-}IC_3H_6SiCl_3$ coupling layer shows a single I $3d_{5/2}$ peak at 620.3 eV for the propyl iodide functionality, the bilayer structure with the $3\text{-}IC_3H_6SiCl_3$ coupling layer and the 4-*N*,*N*-bis(hydroxyethylamino)stilbazolium chromophore layer exhibits two distinct I $3d_{5/2}$ peaks at 620.3 and 618.2 eV (Figure 5b). These two peaks can be assigned to unquaternized propyl iodide and quaternized stilbazolium iodide anion, respectively.[12] The integration of these two peaks provides further information on the quaternization process: the two peaks at 620.3 and 618.2 eV have an intensity ratio of ~1:9. This indicates that ~90% of the propyl iodide functionalities comprising the coupling layer have undergone reaction with 4-*N*,*N*-bis(hydroxyethylamino)stilbazole to form the anchored 4-*N*,*N*-bis(hydroxyethylamino)stilbazolium iodide chromophore on the surface. This extent of quaternization is very reasonable since the molecular bulk of the 4-*N*,*N*-bis-(hydroxyethylamino)stilbazolium chromophore is considerably larger than that of the $3\text{-}IC_3H_6SiCl_3$ coupling agent, and complete quaternization of the packed surface propyl iodide groups does not appear to be physically (sterically) possible. These results are further supported by N 1s XPS spectra (Figure 5c): while the coupling monolayer sample exhibits no N 1s peak, the bilayer structure with both coupling agent and 4-*N*,*N*-bis(hydroxyethylamino)stilbazolium chromophore exhibits two equal-intensity N1s signals at 399.5 and 401.6 eV, which correspond to the amino and pyridinium nitrogen centers, respectively.[12]

Finally, X-ray fluorescence was used to determine the absolute Br coverage in samples **1** and **3** (see Table 1). The anion coverage of 2.5 (0.5) $\times$ 10^{14} Br^-/cm^2 is in excellent agreement with the cation chromophore surface density calculated from second harmonic generation results, 2 (1) $\times$ 10^{14} molecules/cm^2.[5d] This coverage also compares favorably with that determined by second harmonic generation techniques for LB films containing similar chromophores.[16]

Conclusions

Long-period X-ray standing waves have been used for the first time to metrically characterize self-assembled mono- and multilayers. We have applied this to a study of siloxane-based chromophoric multilayers. Both TER-XSW and Bragg-XSW results indicate that Br atoms in these self-assembled multilayers are relatively well-ordered along the surface normal direction. In contrast, our previous attempts to observe synchrotron in-plane X-ray diffraction by these self-assembled multilayers failed, presumably because these multilayers lack extensive in-plane ordering.[17] The present conclusions are further supported by AFM and XPS studies on these SAMs and clearly demonstrate the usefulness of XSWs as a chemically-sensitive, microstructural probe for self-assembled mono- and multilayers, especially for the SAMs with incommensurate structures. We are currently studying anion-exchanged chromophoric multilayers with XSWs to correlate the anion location and second harmonic response.

Acknowledgment. This research was supported by NSF through the Northwestern Materials Research Center (DMR9120521), by ONR-MURI (N00014-95-1-1319), by DOE (DE-FG02-96ER45588), and by DOE through Argonne National Laboratory (W-31-109-ENG-38) and the National Synchrotron Light Source (DE-AC02-76CH00016). W.B.L. thanks the National Science Foundation for a postdoctoral fellowship.

JA962293V

(16) Ashwell, G. J.; Hargreaves, R. C.; Baldwin, C. E.; Bhara, G. S.; Brown, C. R. *Nature* **1992**, *357*, 393−395.

(17) Malik, A.; Lin, W.; Dutta, P.; Marks, T. J. Unpublished results.